Proceedings of the Canadian Society for Mechanical Engineering International Congress
32nd Annual Conference of the Computational Fluid Dynamics Society of Canada
Canadian Society of Rheology Symposium
CSME-CFDSC-CSR 2025
May 25–28, 2025, Montréal, Québec, Canada

The Existence of Truncation Resonance in TPMS-based Periodic Acoustic Metamaterials

Mohamed Shendy[1], Nima Maftoon[2], Armaghan Salehian[1]
[1]Department of Mechanical and Mechatronics Engineering, University of Waterloo, Ontario, Canada
[2]Department of Systems Design Engineering, University of Waterloo, Ontario, Canada

Abstract—Truncation resonance represents peaks that manifest within the bandgap frequency range of periodic metamaterials. This phenomenon stands in contrast to the general conclusion regarding the absence of peaks within bandgap frequency ranges. Truncation resonance is attributed to finite periodic metamaterials, whereas bandgaps pertain to infinite periodic metamaterials. The present study examined the occurrence of truncation resonance in one-dimensional periodic metamaterials constructed from repeated primitive unit cells, observed within the acoustic spectrum. The investigation was geometric-based, considering 10 periodic metamaterials with different relative densities and number of repeated unit cells. This investigation employed both bandgap data and modal analysis, wherein natural frequencies, modeshapes, and Acoustic Pressure Responses (APRs) were integral components of the modal analysis. Following an analysis of APRs, the study was further inspired to scrutinize the numerator of the modal-solved APR. Through analyzing the APR numerator, this work demonstrated the coexistence of truncation resonance and bandgaps in periodic metamaterials.

Keywords- Acoustic Metamaterials, Bloch's theorem, Modal Analysis, Truncation Resonance, TPMS structures.

I. INTRODUCTION

The field of periodic metamaterials has experienced significant advancements in recent years. This progress is attributed to their manifestation of distinctive properties that are absent in continuous materials. Among these properties are negative Poisson's ratio [1], programmable thermal conductivity [2], and bandgaps [3]. It has been determined that these properties can be customized through modifications in the topology of the periodic metamaterials, rendering them attractive to various industries such as automotive and aerospace.

One of the most important aforementioned properties is the existence of bandgaps in periodic metamaterials. Bandgaps represent frequency ranges where the periodic metamaterials have the capacity to attenuate propagating waves. These bandgaps occur within harmonic spectrums, encompassing elastic, acoustic, and electromagnetic domains [4]. The presence of this attribute enables periodic metamaterials to exert control and manipulation over waves, rendering them promising candidates for filtering applications. This paper centers on the presence of bandgaps in periodic metamaterials. Bandgaps arise from the inherent periodicity of the metamaterials, which is characterized by a fundamental element known as the unit cell. The identification of bandgaps within periodic metamaterials is achieved by solving the governing equation while considering the unit cell as the geometric domain. To effectively encapsulate the bandgaps of corresponding periodic metamaterials, it is necessary to incorporate Bloch's theorem [5]. This technique for identifying bandgaps is computationally advantageous, as it relies solely on the unit cell rather than the entire periodic metamaterial structure. It is important to emphasize that Bloch's theorem presumes an infinite repetition of unit cells in the periodic metamaterials. Periodic metamaterials that exhibit bandgaps within the acoustic spectrum are commonly referred to as acoustic metamaterials, with bandgaps designated as acoustic bandgaps. Earlier research has explored the presence of acoustic bandgaps in various periodic acoustic metamaterial designs and determined that these bandgaps are sensitive to the topology of the metamaterial [6], [7], [8], [9], [10], [11], [12], [13], [14]. This realization has prompted couple of studies to undertake topology optimization of periodic acoustic metamaterials to manifest acoustic bandgaps encompassing a significant portion of the audible frequency range (i.e., 20 Hz to 20 kHz) [13], [14]. The employed optimization techniques were based on exhaustive search methodologies, leading to the discovery of optimal designs for periodic metamaterials within a design space of an order of 10^5 and 10^3. These optimal designs displayed acoustic bandgaps covering 94.4% and 85.8% of the audible frequency range, proposed as promising passive devices for airborne noise attenuation.

The verification of bandgaps in periodic metamaterials is performed through the calculation or measurement of the frequency response of finite periodic metamaterials. Specifically, for the verification of acoustic bandgaps, the Acoustic Pressure Response (APR) is employed. The APR, whether calculated or measured, is anticipated to exhibit significant attenuation within frequency ranges that correspond to the bandgaps. As inferred from the statement above, it is generally expected that there will be an absence of modes (i.e., peaks) within the bandgap ranges in the APR [13]. This assumption has been a common conclusion in research addressing bandgaps within both acoustic and elastic domains. Recently, an investigation into the existence of modes within the elastic bandgap range in finite periodic metamaterials has been conducted [15], [16]. This phenomenon is referred to as truncation resonance. The metamaterials examined in this study were beam and rod-based structures. It was observed that truncation resonance is sensitive to variations in geometrical parameters and boundary conditions. In distinguishing between bandgaps and truncation resonance, it is noted that bandgaps are a function of the infinite periodicity of the metamaterial, whereas truncation resonance is related to the finite periodicity of the metamaterial.

The comprehension of truncation resonance in periodic metamaterials is still in its nascent stages. There remain several gaps in this topic that require attention. Notably, one such gap pertains to the phenomenon's presence within the acoustic spectrum and in metamaterials distinguished by their intricate designs. Therefore, this study aims to address this gap by investigating and elucidating the existence of truncation resonance in periodic acoustic metamaterials that are based on Triply Periodic Minimal Surfaces (TPMSs) based. The motivation for this research arises from our prior investigation, which suggested the potential occurrence of this phenomenon in one of the considered design configurations [14].

This work aims to explore and elucidate the presence of truncation resonance within primitive strut-based one-dimensional periodic acoustic metamaterials. This investigation examines 10 designs of metamaterials, which have different relative density (i.e., porosity rate) and the number of repeated unit cells. The work seeks to comprehend the existence of these phenomena by performing a modal analysis on the selected metamaterial designs.

II. Methodology

A. Primitive Strut-based Design

The primitive strut-based design constitutes one of the two types of structures derived from the primitive level-curve surface.

$$\varphi(x,y,z)_P = \cos\left(\frac{2\pi x}{C}\right) + \cos\left(\frac{2\pi y}{C}\right) + \cos\left(\frac{2\pi z}{C}\right) = -t \quad (1)$$

Equation 1 delineates the primitive level curve surface equation ($\varphi(x,y,z)_P$). Here, C represents the unit cell dimension, and t acts as a variable controlling the porosity of the resultant structure. A strut-based structure is realized by filling the cubic volume within the enclosed regions satisfying $\varphi(x,y,z) > t$. The selected geometrical parameter for these structures is the relative density, defined as the rate of porosity. Consequently, a relation between the variable (t) and the relative density is utilized.

$$\rho^*_{ST_P}(t) = 0.2863t + 0.5 \qquad 0.25 \le \rho^*_{ST_P} \le 0.75 \quad (2)$$

Equation 2 illustrates a relation between the relative density and the variable (t) along with a design constraint presenting the range of possible relative densities. Where $\rho^*_{ST_p}$ denotes to the relative density of the primitive strut-based unit cell design. This equation is a polynomial curve-fitted based and was found by one of the earlier efforts [17].

The unit cells examined in the current study are primitive strut-based structures with relative densities varying from 30% to 70%, incrementing by 10% relative density. The unit cell sizes (C) for each were determined based on the size that would facilitate the highest bandgaps coverage within the audible frequency range (i.e., 20 Hz to 20 kHz). Figure 1 depicts the solid and air unit cells of the primitive strut-based unit cells under consideration.

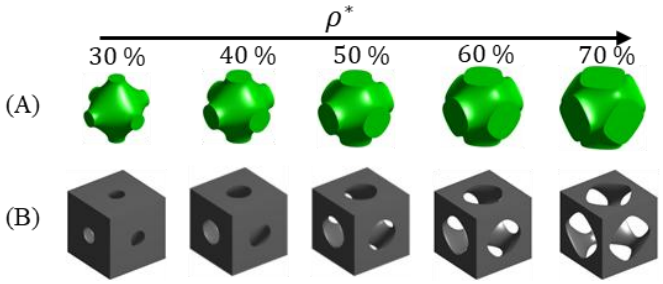

Figure 1 The considered primitive strut-based unit cells. A) Solid Unit Cells. B) Air Unit Cells.

B. Bandgaps Determination

This work focuses on the investigation of the presence of truncation resonance in a one-dimensional periodic acoustic metamaterial constructed from primitive strut-based unit cells. Specifically, the presence of truncation resonance is examined within these metamaterials across the acoustic spectrum. Consequently, it is imperative to ascertain the acoustic bandgaps exhibited by these metamaterials. The determination of bandgaps in these metamaterials was achieved by utilizing the collected normalized bandgap data from our previous study [14]. It is noteworthy that bandgaps were identified by considering the unit cell of the periodic metamaterial through the application of Bloch's theorem. The prior study had computed the normalized bandgap data by employing the FE-Bloch's theorem, with normalization being performed with respect to the unit cell size (C). An assumption of impedance mismatch was made, whereby sound primarily propagates through the air component of the metamaterial, thus leading to the consideration of the air unit cells as the geometrical domain for computing the bandgaps (refer to Figure 1-B). This research leverages the normalized bandgap data to calculate the actual

bandgaps of the considered unit cell designs with specific unit cell sizes (i.e., optimal ones).

$$n = \frac{fC}{c} \tag{3}$$

Equation 3 present the relation between the normalized frequency and its actual counterparts. Where n is the normalized frequency and f is the actual frequency in Hz. c is the speed of sound for the medium (i.e., air medium). The speed of sound considered for this work is equal to $c = 343\ m/s$. This equation is used to convert the normalized bandgaps into their actual counterparts through plugging in different unit cell sizes (C).

The optimal unit cell sizes (C) of the evaluated designs were determined based on those that provided the highest bandgaps coverage within the audible frequency range (i.e., 20 Hz to 20 kHz). The optimization technique employed was the exhaustive search method, which has been utilized in our previous studies. Comprehensive details on the steps of this optimization method are documented elsewhere [13]. Following the application of this exhaustive search, the optimal unit cell sizes (C) and actual bandgaps of the chosen designs were identified. It is essential to emphasize that the aforementioned procedure was carried out to facilitate a more effective visualization of the conducted analysis.

C. The Modal Analysis of the Periodic Metamaterial

The modal analysis of the one-dimensional periodic metamaterial, derived from the examined primitive strut-based unit cell configurations, was performed to provide a comprehensive understanding of truncation resonance existence together with the bandgaps. In this study, modal analysis pertains to the computations of natural frequencies, modeshapes, and Acoustic Pressure Responses (APRs). This analysis can be succinctly described in the following steps. First, the eigenvalue problem is identified and solved.

$$(\omega^2 M + K)P = 0 \tag{4}$$

Equation 4 delineates the Finite Element (FE) discretized eigenvalue problem for the sound wave propagation Partial Differential Equation (PDE) (i.e., commonly referred to as Helmholtz equation). Here, P denotes to the acoustic pressure, ω denotes to the natural frequencies. M, K are the mass and stiffness matrices. This equation is solved to find both the natural frequencies and modeshapes. Second, the APRs are computed through the FE-modal solver. This method utilizes the computed natural frequencies and modeshapes to find the APRs and is known for its computational efficiency.

$$P_s(S) = \sum_{i_m=1}^{i_m=n_m} \frac{|P_{m_s}^{i_m} * \sum P_{m_a}^{i_m}|}{S^2 + (\omega^{i_m})^2} F(s) \tag{5}$$

Equation 5 delineates the modal-based APRs within the frequency domain. Herein, P_s refers to the acoustic pressure at the sensing location. The modeshapes at the sensing and actuation locations are denoted by P_{m_s} and P_{m_a} respectively. F signifies the externally applied sound pressure, while S denotes the frequency domain. The variables i_m and n_m correspond to the mode numbers and the total of mode numbers accounted for. The modeshapes are normalized relative to the mass matrix (i.e.,$\left(P_m^{i_m}\right)^T M\left(P_m^{i_m}\right) = 1$) .It is pertinent to emphasize that this equation embodies the APR in scenarios where the actuation source is distributed across multiple points rather than one point. The considered actuation source is an impulse sound pressure with the magnitude of ($P = 1\ Pa$) and is applied throughout the audible frequency range. For the scope of this study, the actuation points consist of all nodes situated at one end of the metamaterial along its length, while the sensing point constitutes a node positioned at the opposite end. For further clarification, Figure 2 depicts the actuation and sensing scenario pertinent to the metamaterial. A supplementary analysis of the APR, focused on evaluating the numerator of Equation 5, entails the product of the modeshapes at both the sensing and actuation locations (i.e., $|P_{m_s}^{i_m} * \sum P_{m_a}^{i_m}|$). This analysis aids in extrapolating the correlation between truncation resonance and bandgaps, which will be expounded in the subsequent section.

Equation 5 is solved employing the FE commercial software ABAQUS via the utilization of the LANCZOS SOLVER [18] within the FREQUENCY STEP. A mesh sensitivity analysis was conducted, revealing that the solutions exhibit convergence with the element size distribution ranging from 3 mm for maximum to 0.5 mm for minimum dimensions.

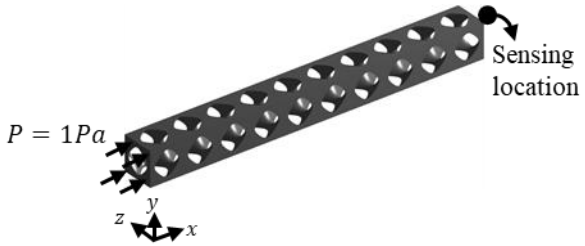

Figure 2 An Illustrative example on the sensing and actuation points considered for this work.

III. RESULTS AND DISCUSSION

A. The Optimal Unit Cell Sizes

The optimal unit cell sizes (C) for each design considered was found using the previously utilized exhaustive search. Table 1 lists down the unit cell designs considered along with their geometrical parameters (ρ^*, C) and bandgaps coverage. One-dimensional periodic acoustic metamaterial made from repeating these unit cells 10 and 20 times were considered. The rationale for varying the number of repeated unit cells within each design was to investigate the sensitivity of truncation resonance in relation to this parameter, concurrently with variations in relative density (ρ^*). Specifically, both the relative density (ρ^*) and the number of repeated unit cells serve as geometrical parameters for examining the presence of truncation resonances in these metamaterials. Subsequent to the consideration of these geometrical variations, 10 one-dimensional periodic acoustic metamaterials are considered.

Table 1 The optimal unit cell sizes along with the bandgaps coverage for the considered unit cell designs.

ρ^* (%)	C (mm)	Bandgaps Coverage (%)
30	10	36.06
40	10.7	45.44
50	11.3	52.95
60	11.9	59.68
70	12.9	68.53

B. Truncation Resonance Analysis

The truncation resonance is examined in the considered one-dimensional periodic metamaterials through the following aspects: the bandgaps, the natural frequencies within the bandgaps region, the APR, and the numerator of the APR (i.e., $|P_{m_s}^{im} * \sum P_{m_a}^{im}|$).

Figure 3 illustrates the bandgaps-structure along with the corresponding natural frequencies (ω_n) residing within the bandgap range for the evaluated 10 metamaterials. Upon examination of this figure, it is evident that all the metamaterials exhibit natural frequencies positioned within their respective bandgap ranges, thereby indicating the presence of truncation resonance. Varying the number of unit cells did not mitigate the truncation resonance in the metamaterials but instead resulted in closer spacing between adjacent natural frequencies as it got increased. This outcome is logical, considering that the length of the structure is inversely related to the natural frequency. Furthermore, an increase in relative density (ρ^*) led to partially diminishing the presence of truncation resonance in these metamaterial designs.

Figure 4 presents the APRs of the considered metamaterials with respect to the actuation and sensing locations depicted in Figure 2. Upon analysis of this figure, it is evident that peaks are observable within the bandgap frequency range, reflecting the presence of modes in this region. However, a comparison of the Sound Pressure Level (SPL) between peaks situated within and outside the bandgap range reveals attenuations within the bandgap frequency range. This observation serves as a proof of concept for the existence of bandgaps in these periodic metamaterials. The underlying reason for the presence of attenuated peaks within the bandgap frequency ranges warrants further investigation. The governing equation of the modal-solved APR is contingent upon the natural frequency (i.e., the denominator in Equation 5) and the product of modeshapes (i.e., the numerator in Equation 5). Attenuation is expected to occur as the numerator value diminishes. Consequently, this study focuses exclusively on analyzing the APR numerator (i.e., $|P_{m_s}^{im} * \sum P_{m_a}^{im}|$). Figure 5 illustrates the APR numerator of the considered metamaterials. Examination of Figure 5 reveals a distinct decrease in the numerator for modes located within the corresponding bandgap frequency ranges (see Figure 3). This finding substantiates that the attenuation in SPL within the bandgap frequency range results from the reduced numerator values. The depiction of the modal-solved APR numerator contributed to a more robust proof of concept for the existence of bandgaps in these periodic metamaterials. Furthermore, it demonstrated that both truncation resonance and bandgaps exist in the periodic metamaterials, and that Bloch's theorem accurately predicts regions of attenuation.

Bloch's theorem predicts the bandgaps of a periodic metamaterial by considering the unit cell as the geometrical domain. Typically, these bandgaps represent frequency ranges wherein the modes are absent for the periodic metamaterial. This was the prevailing understanding among researchers when examining the existence of bandgaps in periodic metamaterials. Recently, *Rosa et al.* and *Park et al.* investigated several periodic beams and rods that exhibited truncation resonance in the elastic spectrum [15], [16]. This current work builds upon these studies by expanding the comprehension of truncation resonance within the acoustic spectrum of complex designs. Additionally, this study demonstrated that both phenomena, namely bandgaps and truncation resonance, coexist within periodic metamaterials. Such a demonstration was unattainable until the modal-solved APR was solved and its numerator analyzed independently, highlighting the significance of modal analysis in periodic metamaterials. The aforementioned paragraphs delineate the contributions of this work.

IV. CONCLUSION

This work has elucidated the existence of truncation resonances in one-dimensional periodic acoustic metamaterials composed of tessellated primitive strut-based unit cells within the acoustic spectrum. The framework of this work can be broadly divided into two stages. The first stage involved calculating the bandgaps of the specified unit cell designs through utilizing the previous normalized bandgaps data. Subsequently, the second stage entailed conducting a modal analysis of the one-dimensional periodic acoustic metamaterials. The elements extracted of this modal analysis encompassed natural frequencies, modeshapes, and APR. Both the natural frequencies and APR revealed the presence of modes within the bandgap range of these periodic metamaterials, thereby attesting to the presence of truncation within these structures. Visualization of the APRs indicated that the peaks situated within the bandgap frequency range exhibited attenuated SPL in comparison to those located outside these ranges. This finding prompted further analysis of the modal-solved APR by examining its numerator (i.e., $|P_{m_s}^{im} * \sum P_{m_a}^{im}|$). The APRs numerator demonstrated a notably reduced value in regions corresponding to the bandgap's range. This led to the conclusion that truncation resonance and bandgaps coexist within the periodic metamaterials.

This work has offered new insights on understanding the coexistence of truncation resonance and bandgaps within the acoustic spectrum of periodic metamaterials. The analyses undertaken in this work are indispensable supplementary tools that should be considered when designing acoustic metamaterials aimed at attenuation, filtering, and sensing applications.

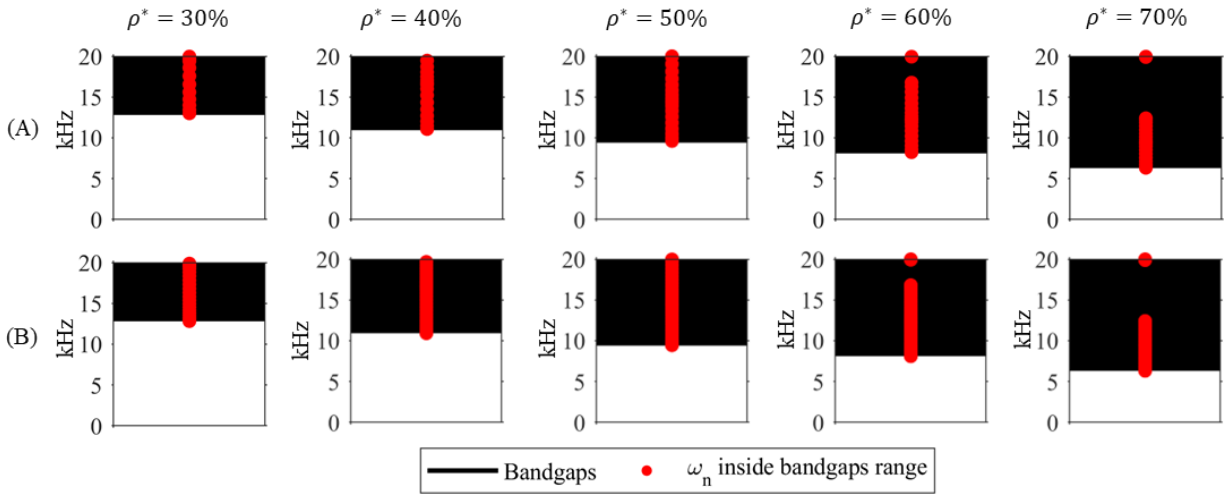

Figure 3 Bandgaps-structure along with the natural frequencies located in the bandgaps regions for the considered one-dimensional periodic metamaterials. A) One-dimensional periodic metamaterials with 10 repeated unit cells. B) One-dimensional periodic metamaterials with 20 repeated unit cells.

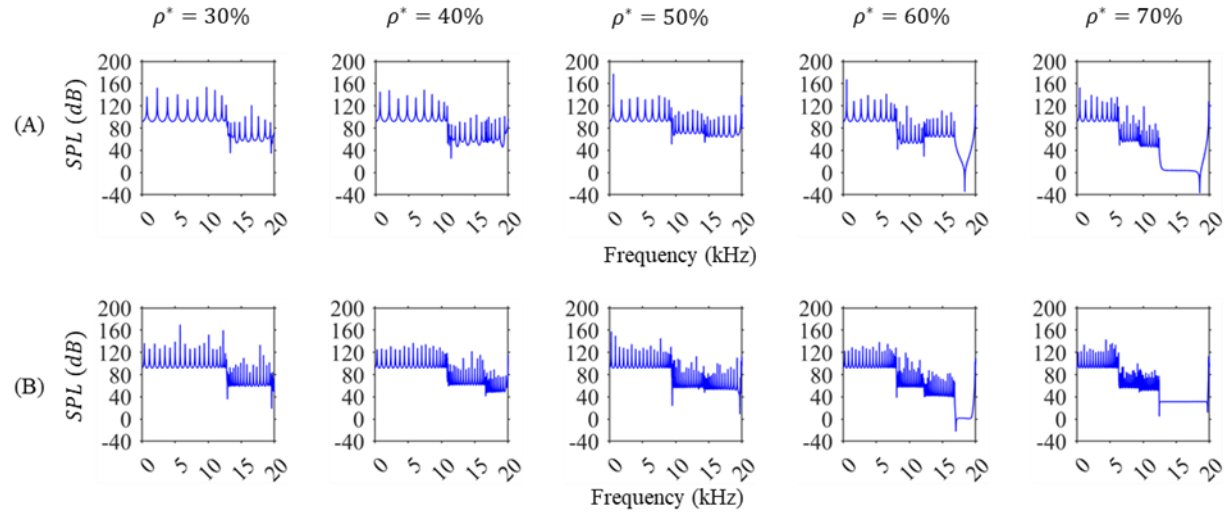

Figure 4 The APR for the considered one-dimensional periodic metamaterials in the selected actuation and sensing conditions. A)One-dimensional periodic metamaterials with 10 repeated unit cells. B)One-dimensional periodic metamaterials with 20 repeated unit cells.

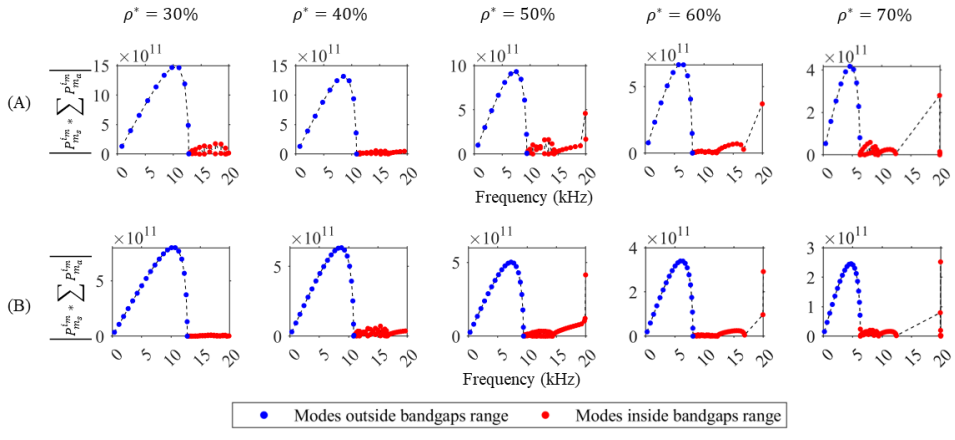

Figure 5 The numerator of the APR for the considered one-dimensional periodic metamaterials. A) One-dimensional periodic metamaterials with 10 repeated unit cells. B) One-dimensional periodic metamaterials with 20 repeated unit cells.

ACKNOWLEDGMENT

This research received funding from both Natural Sciences and Engineering Research Council of Canada (CRDPJ 524018- 18 and RGPIN-2022-03338) as well as the Government of Canada through the Federal Economic Development Agency for Southern Ontario (FedDev Ontario) in the Waterloo Institute for Sustainable Aeronautics at the University of Waterloo (WISA 53072-10071). This work was partially conducted using the High-Performance Computing devices through the use of Digital Alliance of Canada services.

REFERENCES

[1] D. Mousanezhad *et al.*, "Hierarchical honeycomb auxetic metamaterials," *Sci Rep*, vol. 5, Dec. 2015, doi: 10.1038/srep18306.

[2] D. M. Bragin, A. I. Popov, and A. V. Eremin, "The thermal conductivity properties of porous materials based on TPMS," *Int J Heat Mass Transf*, vol. 231, Oct. 2024, doi: 10.1016/j.ijheatmasstransfer.2024.125863.

[3] A. S. Phani, J. Woodhouse, and N. A. Fleck, "Wave propagation in two-dimensional periodic lattices," *J Acoust Soc Am*, vol. 119, no. 4, pp. 1995–2005, Apr. 2006, doi: 10.1121/1.2179748.

[4] Kittel. Charles, *Introduction to solid state physics* , 7th ed. New York: Wiley, 1996.

[5] L. Brillouin, *Wave Propagation in Periodic Structures: Electric Filters and Crystal Lattices*. in Dover phoenix editions. Dover Publications, 2003. [Online]. Available: https://books.google.ca/books?id=m2WmGiU5nUwC

[6] M. Kheybari, C. Daraio, and O. R. Bilal, "Tunable auxetic metamaterials for simultaneous attenuation of airborne sound and elastic vibrations in all directions," *Appl Phys Lett*, vol. 121, no. 8, Aug. 2022, doi: 10.1063/5.0104266.

[7] O. R. Bilal, D. Ballagi, and C. Daraio, "Architected Lattices for Simultaneous Broadband Attenuation of Airborne Sound and Mechanical Vibrations in All Directions," *Phys Rev Appl*, vol. 10, no. 5, Nov. 2018, doi: 10.1103/PhysRevApplied.10.054060.

[8] W. Elmadih, D. Chronopoulos, and J. Zhu, "Metamaterials for simultaneous acoustic and elastic bandgaps," *Sci Rep*, vol. 11, no. 1, Dec. 2021, doi: 10.1038/s41598-021-94053-3.

[9] D. W. Abueidda, I. Jasiuk, and N. A. Sobh, "Acoustic band gaps and elastic stiffness of PMMA cellular solids based on triply periodic minimal surfaces," *Mater Des*, vol. 145, pp. 20–27, May 2018, doi: 10.1016/j.matdes.2018.02.032.

[10] Y. Guo, M. I. N. Rosa, and M. Ruzzene, "Topological Surface States in a Gyroid Acoustic Crystal," *Advanced Science*, vol. 10, no. 6, Feb. 2023, doi: 10.1002/advs.202205723.

[11] Y. Chen, H. Yao, and L. Wang, "Acoustic band gaps of three-dimensional periodic polymer cellular solids with cubic symmetry," *J Appl Phys*, vol. 114, no. 4, Jul. 2013, doi: 10.1063/1.4817168.

[12] Y. Guo, M. Ruzzene, and M. Rosa, "Gyroid-based acoustic materials and devices," 20240029698A1, Jan. 25, 2024

[13] M. Shendy, M. Oluyemi, N. Maftoon, and A. Salehian, "An Extensive Parametric Analysis and Optimization to Design Unidimensional Periodic Acoustic Metamaterials for Noise Attenuation," *Applied Sciences (Switzerland)*, vol. 14, no. 16, Aug. 2024, doi: 10.3390/app14167272.

[14] M. Shendy, N. Maftoon, and A. Salehian, "TOPOLOGY OPTIMIZATION OF ONE-DIMENSIONAL PERIODIC ACOUSTIC METAMATERIAL FOR AIRBORNE NOISE ATTENUATION," in *Proceedings of the ASME 2025 44 International Conference on Ocean, Offshore and Arctic Engineering*, 2025.

[15] M. I. N. Rosa, B. L. Davis, L. Liu, M. Ruzzene, and M. I. Hussein, "Material vs. structure: Topological origins of band-gap truncation resonances in periodic structures," *Phys Rev Mater*, vol. 7, no. 12, Dec. 2023, doi: 10.1103/PhysRevMaterials.7.124201.

[16] S. Park, R. F. Yan, and K. H. Matlack, "Characteristics of truncation resonances in periodic bilayer rods and beams with symmetric and asymmetric unit cells," *J Acoust Soc Am*, vol. 155, no. 2, pp. 791–802, Feb. 2024, doi: 10.1121/10.0024610.

[17] W. Xu, P. Zhang, M. Yu, L. Yang, W. Wang, and L. Liu, "Topology Optimization Via Spatially-Varying TPMS," *IEEE Trans Vis Comput Graph*, 2023, doi: 10.1109/TVCG.2023.3268068.

[18] L. Cornelius, "lanczos1950," *J Res Natl Bur Stand (1934)*, vol. 45, no. 4, pp. 255–282, 1950.